Non-Linear Finite Element Modelling of Anatomically Detailed 3D Foot Model

P. J. Antunes[1*], G. R. Dias[1], A.T. Coelho[2], F. Rebelo[3] and T. Pereira[4]

[1] *IPC – Institute for Polymers and Composites, University of Minho, Guimarães, Portugal*
[2] *AIS – Amorim Industrial Solutions, Corroios, Portugal*
[3] *Ergonomics Laboratory, Faculty of Human Kinetics, Technical University of Lisbon, Lisbon, Portugal*
[4] *The Health Sciences School, University of Minho, Braga, Portugal*

**corresponding author: pantunes@dep.uminho.pt*

KEYWORDS: Hyperelasticity, Strain Energy Function, Finite Element Analysis, Contact Pressure, 3D Foot Model, Shoe Insoles, CT Scan.

SUMMARY: A 3D anatomically detailed non-linear finite element analysis human foot model is the final result of density segmentation 3D reconstruction techniques applied in Computed Tomography (CT) scan DICOM standard images in conjunction with 3D Computer Aided Design (CAD) operations. Density segmentation techniques were used to geometrically define the foot bone structure and the encapsulated soft tissues configuration. CAD modelling was applied for geometrical definitions of cartilages and volumes boolean operations. The monitoring of the contact pressure values at the foot plantar area assumes a vital role on the human comfort optimization of shoe insoles. The contact pressure distribution at the foot plantar area and stresses at the bone structures are calculated for this article only for a rigid contact between the plantar foot area and the rigid ground support. Linear and non-linear elastic constitutive material models were implemented to mechanically characterize the behaviour of the biological materials. Furthermore, preliminary numerical results for the model qualitative evaluation are presented.

1. INTRODUCTION

Finite element analysis can be a very powerful tool in the foot biomechanical study, namely in the stiffness shoe insoles optimization. The human foot comfort can be related with the contact pressure generated at the plantar/insole(soil) interface. Large values of contact pressure can generate pain or pathologies due to the obstruction of blood circulation in areas with peak values of pressure. The foot bone structure supports the weight applied during balanced standing and the soft tissues accommodate deformation that minimizes the contact pressure values. The minimization of contact pressures at the foot plantar area is due to an increase in the contact area values. The comfort enhancement at the foot can be achieved by the application of shoe insoles that must be mechanically optimized to simultaneously support the body weight without foot deviations and act as contact pressure reducers in the precarious plantar zones. The geometrical complexity of the foot structure implies the use of reverse engineering tools in order to obtain a model that can accurately simulate the biomechanical behaviour of the human foot, namely soft tissues and bone structure. This article describes the methodology applied in the development of an anatomically detailed three-dimensional foot model for non-linear finite element analysis from medical image data obtained from a CT scan.

2. 3D MODELLING METHODOLOGY

The complex mechanical behaviour of the foot and the necessity of obtaining accurate results for posterior validation with experimental values implies a adequate modelling of the foot structure in terms of 3D anthropometrical characteristics and material constitutive modelling. The initial step concerning the foot anthropometrical definition was a CT scan of the foot region of a 26 years old male in a Phillips® Brilliance CT equipment. The DICOM images generated in the CT scan were then processed with a medical imaging and editing software (MIMICS® 9.1) that was used to obtain the primary 3D models using density segmentation techniques. The generated primary 3D models were then exported as geometrical files for a CAD system (CATIA®) that allowed the assembly and some 3D geometrical operations. Finally, the CAD model was exported to a non-linear FEM/FEA package (ABAQUS® 6.6.1). The model was then prepared for the non-linear analysis, namely through the definitions of loads, boundary conditions, material constitutive

models, kinematic constraints and mesh discretization processes. The 3D foot modelling methodology is represented in Fig.1.

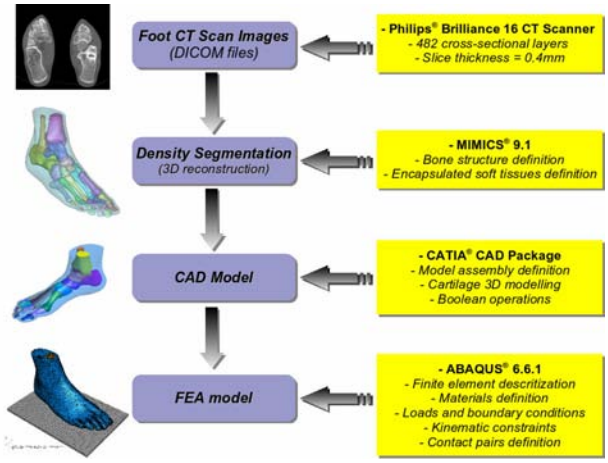

Fig. 1 - Modelling methodology

3. MEDICAL IMAGE DATA GENERATION

A CT scan was performed in a 26 years old male with 75kg weight in a Phillips Brilliance 16 CT equipment. The scan was realized for both foot at the neutral posture in which there is the least tension or pressure on, tendons, muscles and bones and was defined by 482 cross-sectional cuts with a slice distance of 0.4mm and a field of view (FOV) of 346mm. The medical images were exported from the CT equipment in the DICOM format with an image area of 1024x1024 pixels. The high image resolution associated with the reduced distance between slices assures a good geometrical definition of the primary 3D models in the future density segmentation operations.

Fig. 2 - CT Scan equipment

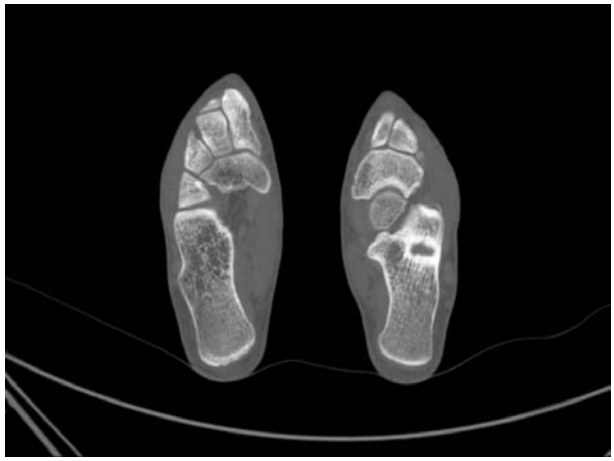

Fig. 3 - CT Scan image

4. DENSITY SEGMENTATION (3D RECONSTRUCTION)

For the reconstruction of the primary 3D anthropometrical models (bone structure and encapsulated soft tissues) was used the MIMICS® 9.1 medical imaging density segmentation software. The DICOM image files generated in the CT scan are constituted by pixels with different gray intensities. The different intensity fields correspond to different material densities presented at the anatomic foot structure, namely, soft tissues, bone and cartilage. Notice that in a CT scan is possible to distinguish also the tendon and ligament structure, but for the present case these structures were not accounted in the 3D reconstruction. The separated 3D reconstruction of each bone segment was accomplished with manual editing operations of the density masks, what allowed the construction of separated masks for each bone present in the bone structure. The reconstruction of the encapsulated soft tissues was faster and easier due to the high difference of densities between the soft tissues and the surrounding air. The spaces between bones normally occupied by cartilages

and sinovial liquid were not segmented. The cartilages were modelled separately in a CAD system witch allowed a posterior region differentiation, necessary for the assignment of different material properties and for the definition of kinematic constraints at the FEA level modelling. The different phases accomplished for the 3D reconstruction using density segmentation techniques with the MIMICS® 9.1 software are presented bellow:

1. Importing the medical data (DICOM images)

The MIMICS software allows the automatic importation of the 482 slice images generated in the CT scan. A pixel size of 0.338mm was automatically calculated accounting the present image resolution (1024x1024 pixels) and the acquisition FOV. The slice distance was correctly determined corresponding to 0.4mm. The pixel size and the slice distance guarantees the coherent dimensional reproducibility of the models generated during the segmentation process. To minimize the project size and maximize the productivity of the 3D reconstruction process, a crop operation was conducted in order to eliminate the slice images of the left foot, concentrating the modelling efforts in the right foot area.

2. Thresholding

Thresholding base on Hounsfield units was used to separate each bone from the bone structure and also for the definition of the encapsulated soft tissues volume. In order to include all the cortical and trabecular bone at the foot bone structure and exclude the cartilage regions, a lower limit of 250HU and an upper limit of 2000HU were defined. The soft tissues region was generated accounting a lower limit of -200HU and an upper limit of 3071HU.

3. Segmentation density masks

For each bone, individual and separated masks were created. This process allows the posterior generation of independent geometrical files and 3D models. Some manual operations to eliminate residual pixels nominally at the cartilages regions and fingers were conducted. Cavity fill operations to rule out some voids at the density masks were also realized in order to obtain independent and smoother primary 3D models. For a better visualization of internal boundaries in the density masks, polylines were generated what allows the use of the *"Cavity Fill from Polylines"* tool, in order to eliminate in an easier way, mask's internal voids.

4. Region growing

The region growing process allows to split the segmentation in different and separated parts, corresponding each part to one mask, that can be distinguished by the different applied mask's colours. For that geometrical separation to happen, the adjacent masks must not be connected with any residual pixel. These operations were performed in all slices generated at the CT scan. For the complete definition of the bone foot structure and soft tissues, 30 different regions were defined.

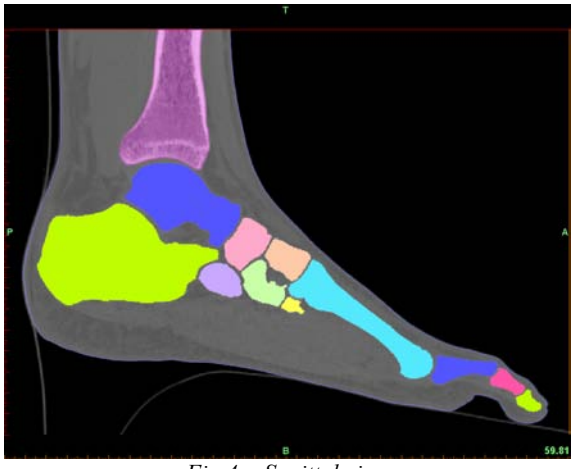

Fig.4 - Sagittal view

Fig. 5 – Coronal view

5. 3D reconstruction

The generated region masks were used to develop 3D models for each the bones and encapsulated soft tissues volume. The 3D reconstruction is based on 3D interpolation techniques that transform the 2D images (slices) in a 3D model. For this reconstruction case, gray values interpolation was used associated with the accuracy algorithm for achieving a more accurate dimensional representation of the foot structure. Shell and triangle reduction, respectively, were used for eliminating small inclusions and reduce the number of the mesh elements. Each region was then reconstructed to obtain all the bones and encapsulated soft tissues volume that geometrically defines the foot structure. Each model was exported to a *.STL file allowing future CAD operations. In Fig. 6 and 7 is possible to see primary 3D models constructed with MIMICS® 9.1 through the medical image data imported from the CT scan.

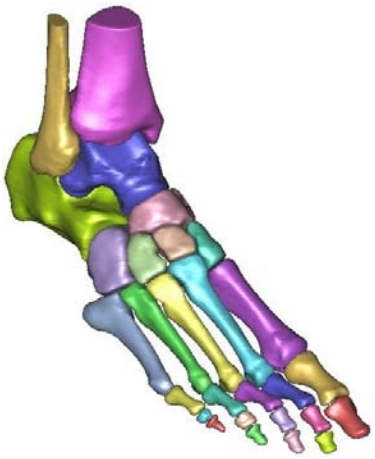

Fig. 6 – Bone structure assembly

Fig. 7 – Soft tissues model

The relative position of the different parts that constitute the primary model assembly and a cross-sectional cut of the foot model are visible in Fig. 8 and 9, respectively.

Fig. 8 – Bone structure + soft tissues assembly

Fig. 9 – Soft tissues section-cut

5. 3D CAD MODELLING

The *.STL files generated in MIMICS® software were imported into CATIA® CAD package. All the parts imported were then assembled together. The cartilages that were not reconstructed in the segmentation process were then modelled in order to connect the bones and fill the cartilaginous space. After the cartilage modelling process, volume boolean operations were performed to achieve a volume of soft tissues that corresponds to the subtraction of the bone structure coupled with the cartilages. This approach, guarantees the perfect alignment of the models exterior surfaces, what is very important to the future finite element model generation. The foot bone structure coupled with the modelled cartilages (Fig. 10) was assembled together with the boolean generated soft tissues volume (Fig. 11).

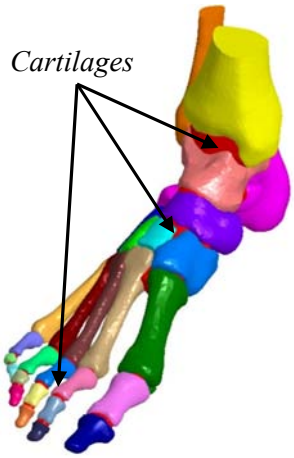

Fig. 10 – Bone structure + cartilages

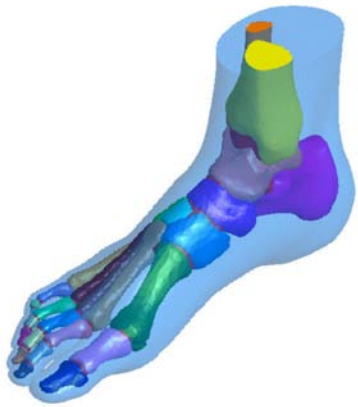

Fig. 11 – Bone structure + cartilages + soft tissues

6. NON-LINEAR FEA MODEL CONSTRUCTION

The finished CAD model was imported and assembled in the non-linear FEA package ABAQUS® 6.6.1. The FEA bone structure model as shown in Fig. 12, consisted of 29 bone parts, that includes all the *distal*, *medial* and *proximal phalanges*, 3 *cuneiforms*, *talus*, *calcaneus*, *cuboid*, *navicular*, *tibia* and *fibula* bones. The bone segments are connected by the cartilage regions modelled in the CAD software.

6.1. Geometrical definition

The encapsulated soft tissues 3D mesh is presented in Fig. 13. The bone and cartilage structure were bonded together forming a unique structure with different material regions. This structure was then bonded to the soft tissues volume, through the definition of mesh tie kinematic constrains.

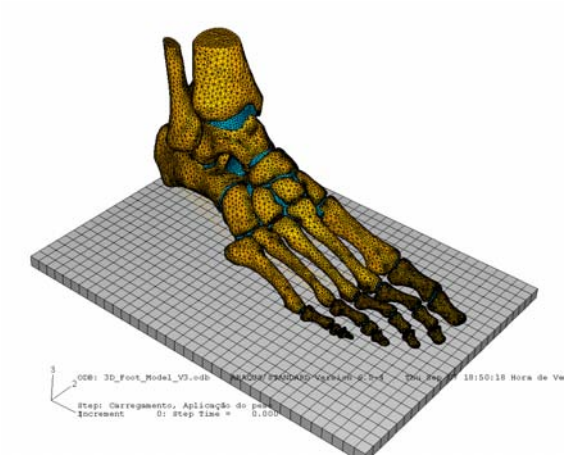

Fig. 12 – Bone structure + cartilages meshes

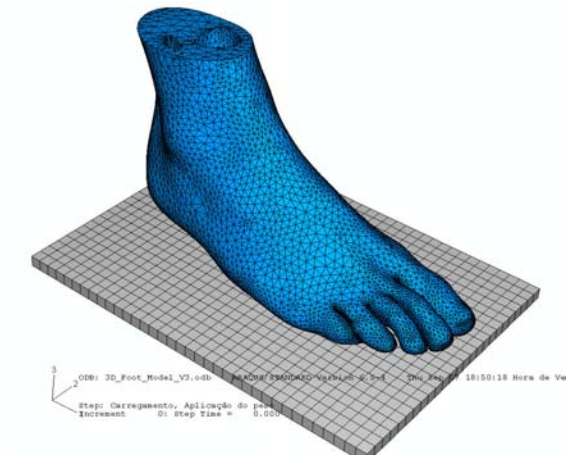

Fig. 13 – Encapsulated soft tissues 3D mesh

The plantar fascia and Achilles tendon were included in the FEA model through the definition of truss and axial connectors elements respectively. The plantar fascia is one of the major stabilization structures of the longitudinal arch of the human foot and sustains high tensions during the weight application [9]. In the FEA model the plantar fascia was geometrically simplified and divided into 5 separated sections (rays). The geometrical definition of the Achilles tendon through axial connector elements, allows the simulation of the load applied in the *calcaneus* zone for a foot during balanced standing. The load at the posterior aspect of the *calcaneus* bone is generated by the involuntary contraction of the triceps surae muscle group in order to stabilize the foot during standing [7]. Six connector elements were defined to simulate the human Achilles tendon. A variety of 3D elements topology and formulations were used to descritize the foot model structure. The foot geometrical complexity do not allows the use of hexahedral elements that usually provides higher accuracy with less computational cost. For that reason, tetrahedral elements that are more versatile to capture

the irregularly shapes of the bone structure and the encapsulated soft tissues, were used to mesh the model. Hybrid element formulation was used to assure the almost-incompressible constrain for the soft tissues non-linear elastic mechanical behaviour. Rigid elements were implemented to define the ground support.

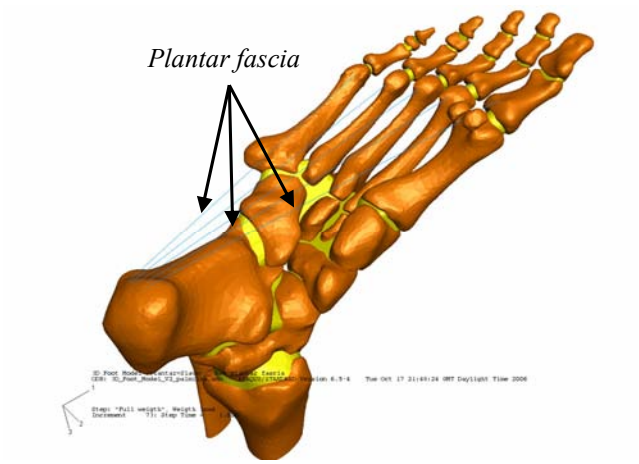

Fig. 14 – Plantar fascia modelling

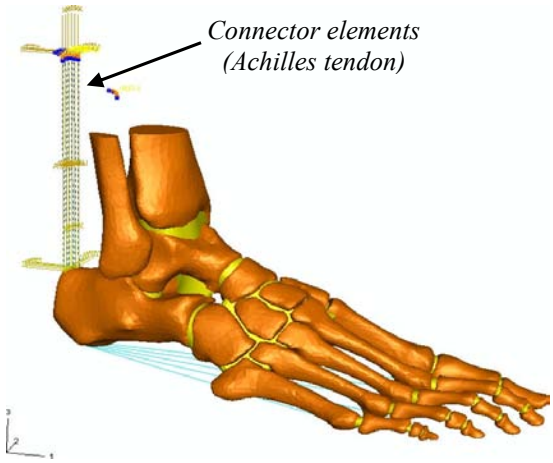

Fig. 15 – Achilles tendon modelling

A horizontal rigid plate was modelled in order to simulate the foot ground support. The foot/ground interface was defined through contact surfaces, what will allow the load transmission between ground support and foot model. The surfaces interaction definition, allows the generation of a contact pressure field at the foot plantar area. A small-sliding tracking approach associated with a node to surface contact formulation was defined to model the interaction tangential behaviour. The foot plantar surface area was defined as the slave surface and the rigid ground support, as the master surface. An Augmented Lagrange constrain enforcement method was implemented in the definition of the interaction normal behaviour. The friction coefficient between the foot and soil was set to 0.6, using the Coulomb friction model [13].

6.2. Loads and Boundary Conditions

A vertical force corresponding to half of the body weight is applied at the ground support reference point. Achilles tendon loads are applied at the end of the axial connector elements for simulating the balanced standing. The value of the Achilles tendon force is not easy to be experimentally measured. For that reason, some analytical assumptions concerning the Achilles tendon load are made in the bibliography, which estimates the Achilles tendon load to be ranging between one half to two thirds the weight applied on the foot. The study of Simkin [12], who calculated that the Achilles tendon force should be approximately 50% of the body load during standing was considered for some foot computational models analysis in the literature [1,7]. The effect of Achilles tendon loading in the standing foot was numerically studied by Cheung et al. [10] who conclude that an Achilles force of 75% of the total weight on the foot provides a closer match to the measured center of pressures at the plantar/ground interface. For a subject with a body mass of 75Kg a vertical reaction force of approximately 375N is generated in each foot. For the present case, two different types of loading were considered. The first case, consider a pure vertical compression load of the foot defined by a vertical force (375N) applied in the ground reference point. The second loading case considers simultaneously the force applied in the *calcaneus* bone through the Achilles tendon and the ground reaction force, in order to simulate the balanced standing. A magnitude of 187.5N was calculated for the Achilles tendon force, following the model of Simkin [12]. The upper surfaces of the soft tissues, *tibia* and *fibula* were fixed through the analysis time via a kinematic constrain, while the boundary conditions applied at the soil reference point load, allowed uniquely the plate movement in the vertical (upper) direction.

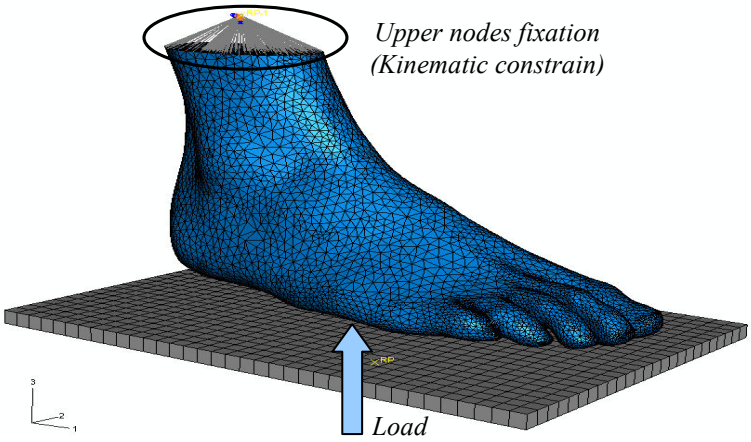

Fig. 16 – Applied load and boundary conditions

6.3. Material Properties

All the materials were considered isotropic and linear-elastic except the soft tissues that are mechanically characterized by a non-linear elastic behaviour. The bone material behaviour was linearly with a Young's Modulus and Poisson's ratio, defined as 7300 MPa and 0.3, respectively. These values were obtained by weighing cortical and trabecular bone elasticity according to Nakamura et al. [5]. The mechanical properties of the cartilage [3, 6], plantar fascia [1], were selected from the literature.

Table 1. Material properties and element topology/formulation

	Element				
Components	***Topology***	***Formulation***	***Young's modulus (MPa)***	***v***	***Cross-sectional area (mm^2)***
Bone structure	3D-Tetrahedra	Linear	7300	0.3	-
Cartilage	3D-Tetrahedra	Linear	10	0.4	-
Soft tissues	3D-Tetrahedra	Linear, Hybrid	Hyperelastic	≈ 0.5	-
Achilles tendon	1D	Axial Connector element	∞	-	-
Plantar fascia	1D	Truss element	350	-	58.6
Soil	Quadrilateral	Rigid element	∞	-	-

Specifically, the bulk soft tissues non-linear elastic mechanical behaviour definition was based on the uniaxial stress-strain data obtained from *in vivo* tests of the heel [2]. This non-linear material definition can model more accurately the soft tissues mechanical behaviour in areas where the soft tissues deformation is higher and for that, not ruled by a linear mechanical response. Although some authors [3] consider the soft tissues as a linear elastic material, the present non-linear mechanical approach can model more accurately the foot mechanical behaviour, namely, the plantar contact pressure field definition.

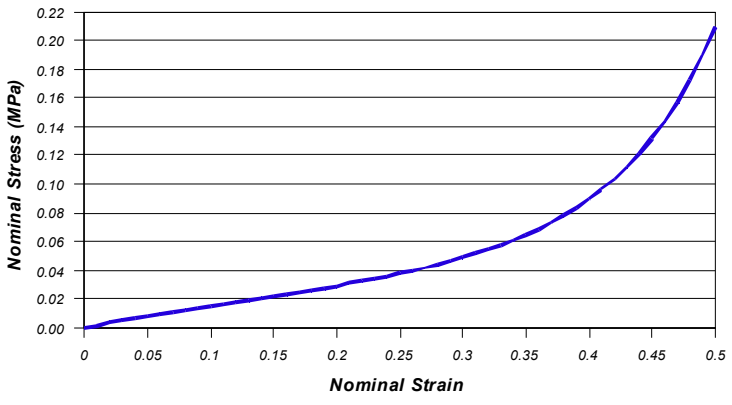

Fig. 17 – Encapsulated soft tissues non-linear uniaxial mechanical behaviour

The bulk soft tissues non-linear mechanical behaviour was defined through a hyperelastic model based on a second order polynomial strain energy function [1, 2], given by the expansion of (1).

$$\omega\left(J,\bar{I}_1,\bar{I}_2\right)=\sum_{i+j=1}^{N}C_{ij}\left(\bar{I}_1-3\right)^i\left(\bar{I}_2-3\right)^j+\omega_{vol}\left(J\right) \quad (1)$$

Setting $N=2$ and considering that the pure volumetric response is given by the strictly convex function: $\omega_{vol}(J)=\frac{1}{D_i}(J-1)^{2i}$, the decoupled second order hyperelastic polynomial model is given by:

$$\omega\left(J,\bar{I}1,\bar{I}2\right)=C_{10}\left(\bar{I}_1-3\right)+C_{01}\left(\bar{I}_2-3\right)+C_{20}\left(\bar{I}_1-3\right)^2+C_{11}\left(\bar{I}_1-3\right)\left(\bar{I}_2-3\right)+C_{02}\left(\bar{I}_2-3\right)^2+\sum_{i=1}^{N}\frac{1}{D_i}(J-1)^{2i} \quad (2)$$

where ω is the overall strain energy per unit of reference volume; J is the volume ratio; C_{ij} and D_i are material parameters obtained from the experimental data; $\bar{I}_1$ and $\bar{I}_2$ are the modified strain invariants. The material parameters used for the definition of the hyperelastic model associated with the non-linear mechanical definition of the soft tissues, are presented in Table 2.

Table 2. - Encapsulated soft tissues hyperelastic material parameters

C_{10}	C_{01}	C_{20}	C_{11}	C_{02}	D_1	D_2
0.08556	-0.05841	0.03900	-0.02319	0.00851	3.65273	0

7. NON-LINEAR FEA PRELIMINARY RESULTS

The anatomically detailed 3D FEA foot model was developed from CT scan images using density segmentation techniques and CAD manipulation. Kinematic constrains between bone structures, cartilages and soft tissues were defined. The load transmission between ground support and the foot structure was defined by the introduction of contact pairs, namely, at the foot plantar area/ground support interface. Large deformations and non-linear geometrical analysis associated with material nonlinearities were considered. The created FEA model allows the output of several results that can be used for comfort evaluation of shoe insoles or to study other biomechanical aspects of the foot. The monitoring of contact pressure values at the foot plantar area assumes a vital role on this study. The following results were obtained considering two different load cases, namely, pure compression load (weight load) and balanced standing load (weight load + Achilles load). The following results are preliminary and are presented only for a qualitative evaluation of the stress and contact pressure fields at the foot structure.

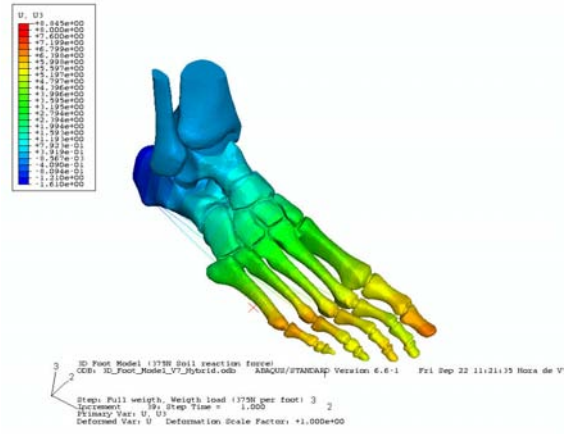

Fig. 18 – Nodal displacement (Pure Compression)

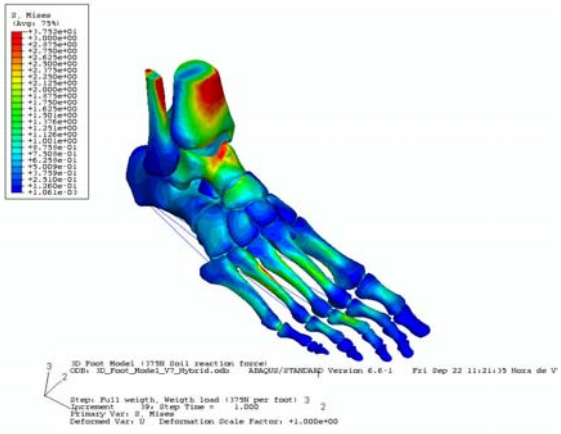

Fig. 19 – Von Mises stress (Pure compression)

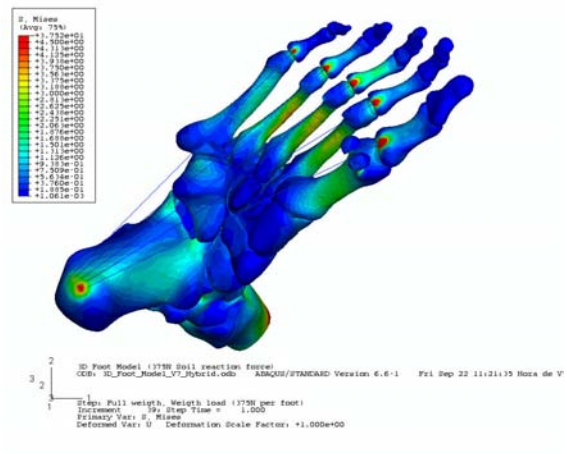

Fig. 20 – Von Mises stress (Pure compression)

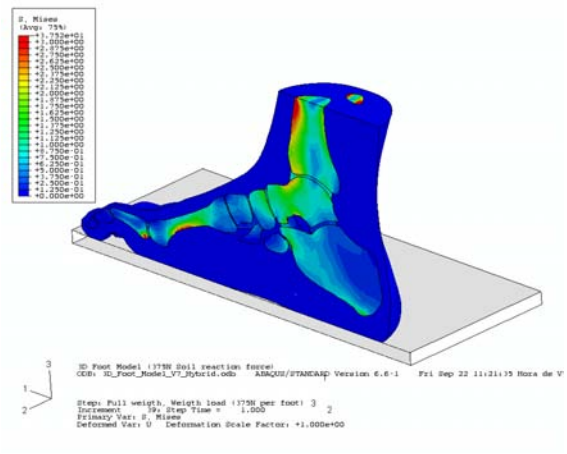

Fig. 21 – Foot section-cut (Pure compression)

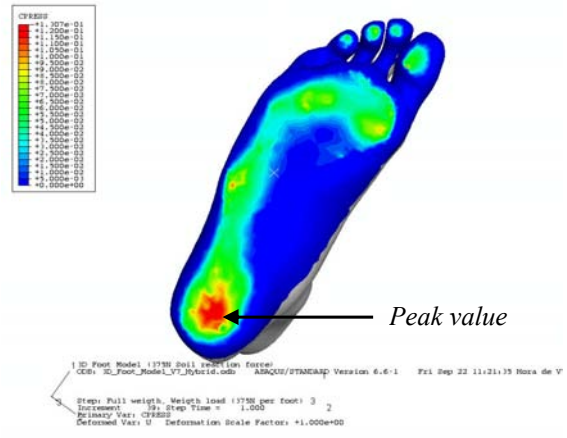

Fig. 22 – Plantar contact pressure (Pure compression)

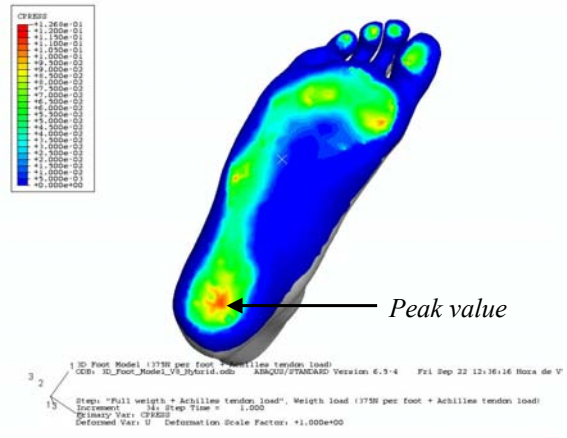

Fig. 23 – Plantar contact pressure (Balanced standing)

The FEA model predicts maximum plantar contact pressure value of 0.131 MPa (13.1 N/cm^2) and 0.108 MPa (10.8 N/cm^2) for the pure compression (Fig. 22) and balanced standing case (Fig. 23), respectively. The contact pressure under the *metatarsal* heads and at the *distal phalanges* increases with the load application at the posterior *calcaneus.* The load at the *calcaneus* compared with the pure compression load, displaces the centre of pressure and increases the load-bearing at the forefoot reducing consequently the load-bearing at the rearfoot. At the bone structure, peak of stress are present at the *metatarsal* and *talus* bones. The insertion points of the fascia plantar truss elements at the *phalanges/metatarsal* connection region and *calcaneus* bone, experienced large stress due to the generated fascia plantar tension (Fig. 20). In Table 3 are presented indicative contact pressure values at the metatarsal head and heel regions.

Table 3. - Contact pressure distribution

Load Case	***1st Metatarsal***	***2st Metatarsal***	***3st Metatarsal***	***4st Metatarsal***	***5st Metatarsal***	***Calcaneus***
Pure compression	0.079 MPa	0.041 MPa	0.072 MPa	0.074 MPa	0.054 MPa	0.131 MPa
Balanced Standing	0.087 MPa	0.049 MPa	0.081 MPa	0.079 MPa	0.060 MPa	0.108 MPa

8. EXPERIMENTAL VALIDATION

The FEA results will be validated by experimental measurements using instrumented pressure insoles from PEDAR® System by NOVEL®. These instrumented pressure insoles allows the dynamic and static measurement of contact pressure values at the foot plantar area. The same male subject that has been submitted to the CT scan will be used for the experimental measurement. Contact pressure values at the hell region and metatarsal heads will be monitored and compared with the FEA results. Experimental contact area values and coordinates of the centre of pressure at the interface region will also be compared with the numerical results.

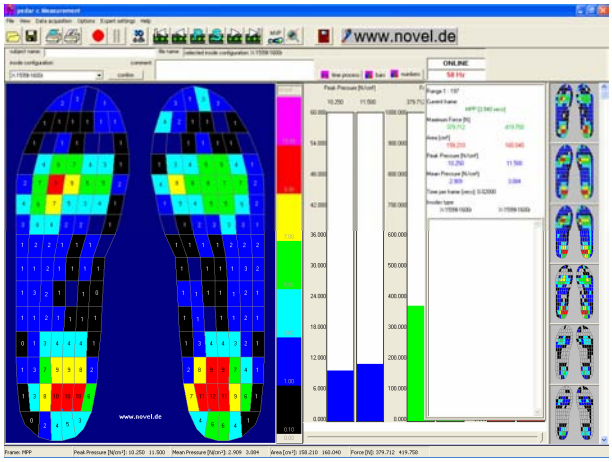

Fig. 24 – Instrumented pressure insoles results output

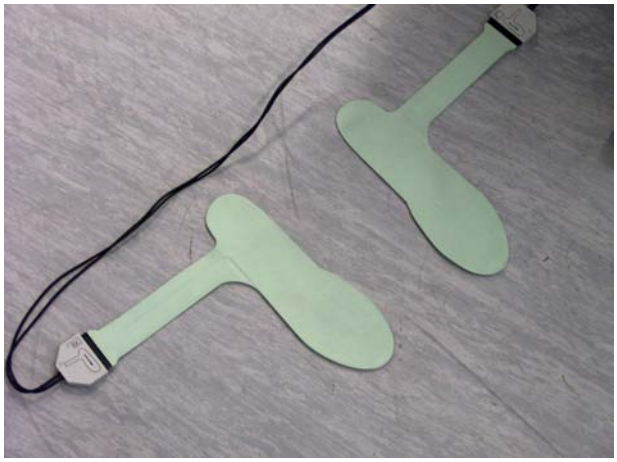

Fig. 25 – Instrumented pressure insoles

9. CONCLUSIONS AND FUTURE WORK

FEA models can be a very powerful method to understand the foot mechanical behaviour and its implications to human comfort generation. This non-linear FEA model intends to be a tool for the design optimization process of shoe insoles. For that purpose, an anatomically detailed foot model was generated from CT scan image data using segmentation reconstruction techniques and 3D CAD modelling. In the present model, several material constitutive models are considered. Kinematic constraints and parts interactions namely at the foot plantar/soil interaction are implemented. Achilles tendon and plantar fascia were introduced considering some geometrical simplifications. The monitoring of plantar contact pressure at the foot plantar area is the main objective. The FEA contact pressure values will be experimentally verified by the use of instrumented pressure insoles. The effect of the magnitude of load at the Achilles tendon will be studied in order to understand its effect on the contact pressure distribution, contact area and coordinates of the centre of pressure. After the conclusion of the experimental verification procedure, a wide variety of insole geometries and insole materials can be tested (Fig. 26) in order to study the comfort foot behaviour through the modification of insole geometrical design and/or insole materials definition.

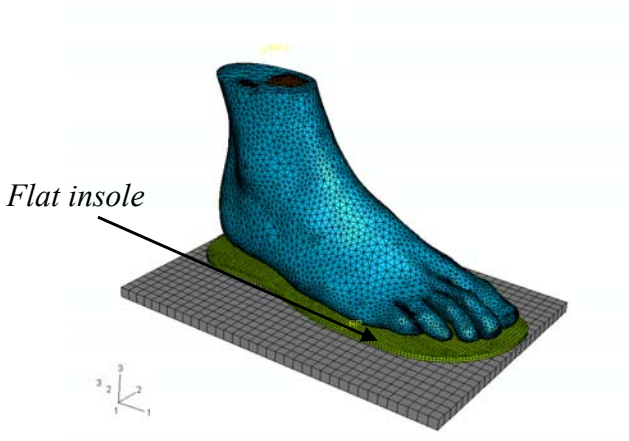

Fig. 26 – Insole implementation on FEA model

10. REFERENCES

[1] Cheung, J.T., Zhang M., Leung, A.K.L., Fan Y.B.; ***Three Dimensional Analysis of the Foot During Standing – A Material Sensitivity Study***; Journal of Biomechanics, 2005.

[2] Lemmon, D., Shiang, T.Y., Hashmi, A.,Ulbrecht, J.S., Cavanagh, P.R.; ***The Effect of Shoe Insoles in Therapeutic Footwear – A Finite Element Approach***; Journal of Biomechanics, 1997.

[3] Shanti, J., Mothiram K. P., ***Three Dimensional Foot Modelling and Analysis of Stresses in Normal and Early Stage Hansen's Disease with Muscle Paralysis***; Journal of Rehabilitation Research & Development, 1999.

[4] Schreppers, G.J.M.A., Sauren, A.A.J.H., Huson, A.; ***A Numerical Model of the Load Transmission in the Tibio-Femoral Contact Area***; Proc Inst Mech Eng(H), 1990.

[5] Nakamura S., Crowninshield R.D., Cooper R.R.; ***An Analysis of Soft Tissue Loading in the Foot: a preliminary report; Bulletin of Prosthetics Research***; 1981.

[6] Gefen, A.; ***Plantar Soft Tissue Loading Under the Medial Metatarsals in the Standing Diabetic Foot***; Medical Engineering & Physics; 2003.

[7] Gefen, A.; ***Stress Analysis of the Standing Foot Following Surgical Plantar Fascia Release***; Journal of Biomechanics, 2002.

[8] Camacho, Daniel L.A., Ledoux, William R., Rohr, Eric S., Sangeorzan, Bruce J., Ching, Randal P.; ***A Three-Dimensional, anatomically detailed Foot Model: A Foundation for a Finite Element Simulation and Means of Quantifying Foot-Bone Position***; Journal of Rehabilitation Research & Development, 2002.

[9] Cheung, J.T., Zhang,M., An, K.N.; ***Effects of Plantar Fascia Stiffness on the Biomechanical Responses of the Ankle-Foot Complex***; Clinical Biomechanics, 2004.

[10] Cheung, J.T., Zhang, M., An, K.N.; ***Effect of Achilles Tendon Loading on Plantar Fascia Tension in the Standing Foot***; Clinical Biomechanics, 2006.

[11] Holzapfel, G.A.; ***Nonlinear Solid Mechanics***; John Wiley & Sons, Ltd., 2005.

[12] Simkin, A.; ***Structural Analysis of the Human Foot in Standing Postur***e; PhD Thesis, Tel Aviv University, 1982.

[13] Zhang, M., Mak, A.F.T.; ***In vivo skin frictional properties***; Prosthetics and Orthotics International, 1999

[14] ABAQUS User's Manual, Version 6.6, 2006.

[15] MIMICS 9.1 Reference Guide, Materialise N.V., 2005.